

AD _____

Award Number: W81XWH-12-1-0492

TITLE: A Stem Cell-Seeded Nanofibrous Scaffold for Auditory Nerve Replacement

PRINCIPAL INVESTIGATOR: Dr. R. Keith Duncan

CONTRACTING ORGANIZATION: University of Michigan
Ann Arbor, Michigan 48109-1274

REPORT DATE: October 2013

TYPE OF REPORT: Annual Report

PREPARED FOR: U.S. Army Medical Research and Materiel Command
Fort Detrick, Maryland 21702-5012

DISTRIBUTION STATEMENT: Approved for Public Release;
Distribution Unlimited

The views, opinions and/or findings contained in this report are those of the author(s) and should not be construed as an official Department of the Army position, policy or decision unless so designated by other documentation.

REPORT DOCUMENTATION PAGE				Form Approved OMB No. 0704-0188	
Public reporting burden for this collection of information is estimated to average 1 hour per response, including the time for reviewing instructions, searching existing data sources, gathering and maintaining the data needed, and completing and reviewing this collection of information. Send comments regarding this burden estimate or any other aspect of this collection of information, including suggestions for reducing this burden to Department of Defense, Washington Headquarters Services, Directorate for Information Operations and Reports (0704-0188), 1215 Jefferson Davis Highway, Suite 1204, Arlington, VA 22202-4302. Respondents should be aware that notwithstanding any other provision of law, no person shall be subject to any penalty for failing to comply with a collection of information if it does not display a currently valid OMB control number. PLEASE DO NOT RETURN YOUR FORM TO THE ABOVE ADDRESS.					
1. REPORT DATE October 2013		2. REPORT TYPE Annual		3. DATES COVERED 30 September 2012-29 September 2013	
4. TITLE AND SUBTITLE A Stem Cell-Seeded Nanofibrous Scaffold for Auditory Nerve Replacement				5a. CONTRACT NUMBER W81XWH-12-1-0492	
				5b. GRANT NUMBER W81XWH-12-1-0492	
				5c. PROGRAM ELEMENT NUMBER	
6. AUTHOR(S) Dr. Robert Duncan, PhD E-Mail: rkduncan@umich.edu				5d. PROJECT NUMBER	
				5e. TASK NUMBER	
				5f. WORK UNIT NUMBER	
7. PERFORMING ORGANIZATION NAME(S) AND ADDRESS(ES) University of Michigan 1058 Wolverine Tower 3003 South State Street Ann Arbor, Michigan 48109-1274				8. PERFORMING ORGANIZATION REPORT NUMBER	
9. SPONSORING / MONITORING AGENCY NAME(S) AND ADDRESS(ES) U.S. Army Medical Research and Materiel Command Fort Detrick, Maryland 21702-5012				10. SPONSOR/MONITOR'S ACRONYM(S)	
				11. SPONSOR/MONITOR'S REPORT NUMBER(S)	
12. DISTRIBUTION / AVAILABILITY STATEMENT Approved for Public Release; Distribution Unlimited					
13. SUPPLEMENTARY NOTES					
14. ABSTRACT The chief aim of our study is restoration of hearing by regeneration of peripheral auditory neurons. The study takes a systematic approach in three objectives aiming to push human stem cells toward an auditory neural fate, embed the cells on a functionalized scaffold, and implant the device in a deafened animal model. In the first year of the project grant, we have addressed three key tasks: (1) derivation of sensory neurons from human pluripotent stem cells (hPSCs), (2) development of implantable nanofibrous substrates, and (3) optimization of the deafness model. In contrast to prior experiments in mouse embryonic stem cells, generation of sensory neurons simply by overexpression of neurogenin-1 in human embryonic stem cells was inefficient. As a result, we have established a small molecule programming strategy for producing sensory glutamatergic neurons that express otic transcriptional programs. These methods will be combined with neurogenin-1 overexpression to optimize derivation of auditory-like neurons. In addition, we developed novel methods for coiling a nanofiber scaffold to maintain the auditory nerve topology and establishing ouabain as an effective chemical tool for destroying endogenous auditory neurons in guinea pigs.					
15. SUBJECT TERMS Human stem cells, neurodifferentiation, deafness model, nanofiber					
16. SECURITY CLASSIFICATION OF:			17. LIMITATION OF ABSTRACT	18. NUMBER OF PAGES	19a. NAME OF RESPONSIBLE PERSON
a. REPORT	b. ABSTRACT	c. THIS PAGE			USAMRMC
U	U	U	UU	16	19b. TELEPHONE NUMBER (include area code)

Table of Contents

	<u>Page</u>
Cover Form	1
Report Documentation Page	2
Table of Contents	3
Introduction	4
Body	4-16
Key Research Accomplishments	4-8
Reportable Outcomes	8
Conclusion	8-9
References	9
Supporting Data (Figures)	10-16

I. INTRODUCTION:

An estimated 300 million individuals world-wide suffer some form of hearing loss, and military personnel exhibit auditory deficits at an exceptionally disproportionate level compared with the lay population. In fact, the ear is the organ most affected by concussive or penetrating injuries to the head. The devastating impact of widespread hearing loss on practical, social, and economic levels drives our interest in devising ways to restore hearing completely. Complete restoration of hearing is a particularly challenging task. In this project, we explore a systematic approach for developing a next-generation auditory prosthesis by replacing damaged auditory nerve with stem cell-derived neurons, grown on a nanofiber substrate, and stimulated by a high-density electrode array. We have divided our research goals into three primary objections. Objective 1 seeks to recapitulate the physiology of auditory neurons using human pluripotent stem cells. In Objective 2, we will develop a mat of aligned nanofibers to guide the arrangement of stem cell-derived neurons to mimic the arrangement as well as the physiology of the auditory ganglion. We also develop the means to electrically stimulate derived neurons on this nanofiber substrate. And finally, in Objective 3, we will implant a prototype device in an animal model of neural hearing loss, examining the capacity for stem cell-derived neurons to functionally integrate with the auditory brainstem.

II. BODY:

A. KEY RESEARCH ACCOMPLISHMENTS

Tasks and deliverables are organized according to the major Objectives in the proposal. Progress on Year 1 tasks is bulleted along with any challenges and recommendations. In some cases, tasks originally scheduled for Years 2-4 were initiated early, and progress is bulleted accordingly. All other tasks are listed as “pending”.

Task 1. IACUC review of animal care and use application. The application is under development and will be submitted prior to any award. We estimate some time for modification of this protocol based on feedback from reviewers (months 1-4)

- University oversight of the project involved animal care and use (IACUC), stem cell committee review (HPSCRO), recombinant DNA review (IBC), human tissue exemption (IRB), and chemical safety review (OSEH). Approvals were obtained from all oversight groups.

Objective 1: Evaluate the combination of genetic and neurotrophic cues on the differentiation of adult hiPSCs toward an auditory nerve-like phenotype (months 1-18)

Task 2. Gene expression analysis using RNA sequencing to compare the transcriptomes of induced cells and native auditory nerve (months 1-12)

- Our initial goal in Year 1 was to establish a reliable, efficient method for pushing human pluripotent stem cells (hPSCs) to an auditory-nerve fate. Indeed, this is the underpinning of all remaining tasks. We began our efforts with human embryonic stem cells (H7 line from WiCell) because these are far simpler to maintain in culture than hiPSCs. Work in Year 2 will transition to the hiPSC line.
- Neurog1 vector design: Our previous work relied on a genetically modified mouse embryonic stem cell line overexpressing neurogenin-1 (Neurog1) (Tong et al., 2010, Hill et al., 2012, Purcell et al., 2012, Purcell et al., 2013), an essential proneural gene in formation of auditory neurons (Ma et al., 2000). As described in the proposal, we have sought methods to overexpress Neurog1 using episomal vectors to prevent insertional mutations and to make the approach broadly applicable and easily transferable. We first established a plasmid vector with an optimal promoter for expression in human stem cells. In a previous study using lentivirus reporters expressed in hESCs, EF1 α was identified as producing the most robust and stable gene expression during differentiation programs (Norrman et al., 2010). We found this to be true as well, when comparing GFP reporter expression in H7 cells transiently transfected with plasmids driven by CAG (chick beta-actin enhancer), CMV, and EF1 α . Even so, plasmids encoding EF1 α .Neurog1.IRES.GFP showed low transfection efficiency (approximately 10% of cells), and

transfected cultures generated about the same number of TUJ1+ neurons as untransfected, control cultures. This result stands in stark contrast to that from our previous work in mouse stem cells, where Neurog1 overexpression efficiently increased the number of cells adopting a neuronal fate. We hypothesized that the degree of Neurog1 overexpression may differentially impact fate specification. To unmask the effects of Neurog1, we selected only the brightest GFP+ cells by flow cytometry and compared these with GFP- cells (Figure 1A-C). The transfected cells showed robust GFP expression even out to 5 days after transfection (Figure 1D) and a larger percentage of TUJ1+ cells projecting neurites over 50% longer than spontaneously differentiated cells. While encouraging, these data were still troubling, in that about the same absolute number of neurons were found in GFP- and GFP+ conditions, suggesting that Neurog1 overexpression may have just biased the cultures toward terminal differentiation. In other words, Neurog1-induction appeared to suppress ongoing proliferation of non-neuronal cells rather than increasing the number of neuronal cells. We next sought methods to increase Neurog1 expression and transfection efficiency using an adenoviral vector. In collaboration with Vector Biolabs, we identified Ad5.RGD as an efficient infection construct capable of infecting ~70% of hESCs and hiPSCs. An expression vector consisting of Ad5.RGD.EF1 α .GFP.2A.Neurog1 was generated (referred to from here forward as Ad5.Neurog1). Though expression efficiency was increased, we still were not able to produce neurons much greater than spontaneous differentiation, when exposing pluripotent stem cells to the virus. We next sought chemical methods to generate glutamatergic, placodal neurons with the goal of combining small molecules and our gene vector to guide hESCs to an auditory fate.

- Stepwise programming with small molecule morphogens: A stepwise protocol for neurodifferentiation was established based on previously published methods (Figure 2A) (Kim et al., 2011). Briefly, embryoid bodies (EBs) are generated by spin-aggregation in Aggrewell-800 micropatterned plates (or Sylgard alternatives, see below) (Figure 2B, C) and pushed toward a neuroectodermal fate using the SMAD-inhibitors noggin and dorsomorphin. On day 2, EBs were plated onto Matrigel and incubated in DMEM/F12 with or without combinations of the morphogens retinoic acid (RA) and sonic-hedgehog agonist purmorphamine (Pur). Though both are required for otic patterning, little is known about how each influences the expression of various proneural basic-helix-loop-helix (bHLH) transcription factors and their downstream placode programs. After formation of rosettes and supplementation by FGF-2, neural precursors are isolated and plated on Matrigel in the presence of Neurobasal with N2 and B27.
- Patterning in high density cultures: To examine the effect of seed density on neurodifferentiation, high density cultures were produced. Neurotransmitter fate and electrophysiology features were similar to low density cultures but several distinct morphologies became apparent after 2-weeks in culture. Many regions with networks of TUJ1+ neurites were seen (Figure 2H) along with regions of fasciculated aggregates (Figure 2I). However, we also observed large 3D, detached aggregates that formed into nets (Figure 2J) or long tubes, up to 1 cm in length in some cases. This is an exciting observation, suggesting progression from stem cell to neuron to nerve. We are pursuing new funding opportunities to further explore these observations and have established connections with clinical faculty in our department to examine regeneration of facial nerve using these structures. Derivation of fasciculated ganglion may also reduce the need for nanofiber substrates in the future.
- Quantitative PCR results: Basic-helix-loop-helix (bHLH) transcription factors, including the neurogenins (Neurog1, Neurog2, Neurog3) and genes such as Ascl1 and Atoh1, are critical in neurogenesis but little is known about how various induction programs affect expression of these factors and their downstream proneural target NeuroD1. Ascl1 and Neurog1 are expressed in SGNs (Hashino and Fritsch, 2011), but Neurog2 and Neurog3 are not necessary for SGN development. SMAD-inhibitors in the EB stage were effective at upregulating all bHLH genes examined (Figure 2K). The morphogens RA and Pur further upregulated these genes with profound effects on Neurog1 and Ascl1, which naturally led to similar increases in the downstream factor NeuroD1. An otic placode transcriptional cascade (Pax2/8, Brn3a, and Gata3) was also upregulated, with Pur showing the largest impact (Figure 2L). Though encouraging, these data do not indicate that an exclusively otic placodal fate was being generated. While Pax2/8 are otic placode markers, Pax6 identifies anterior placodes such as lens and olfactory domains (Schlosser, 2006) that also involve Ascl1 and neurogenin transcriptional

cascades. Pax6 was highly upregulated by our EB and rosette programming, suggesting mixed fates in our neural progenitors.

- Combined Ad5.Neurog1 and small molecule morphogen programming: In a recent report, pre-differentiated stem cells were exposed to several adenoviral vectors to direct motorneuron differentiation (Hester et al., 2011). We explored a similar paradigm, infecting with Ad5.Neurog1 at the neural rosette stage. Single or repeated exposure to the virus dramatically increased Neurog1 expression (100-1000 fold over RA+Pur alone) (Figure 3). The vector has little impact on other bHLH factors but decreased Pax8 expression over 10-fold. This was surprising given Pax8 as a late-stage otic marker and a key factor in auditory nerve development. In the first part of Year 2, we will maximize Neurog1 expression during EB phase, since bHLH genes are already induced at this stage, and re-examine fate specification and rate of maturation of excitable, sensory neurons.
- EB deliverable: In transitioning our studies toward a stepwise protocol, it was necessary to form embryoid bodies. Generation of EBs is notoriously associated with culture heterogeneities because of differences in EB size and shape. Spin-aggregation in using Aggrewell-800 micropatterned culture plates is an efficient and reproducible method for making EBs, but it is extremely expensive. A more recent method that has improved reproducibility relies on forced aggregation in V-shaped agarose casts formed from the Aggrewell original (Dahlmann et al., 2013). We sought to duplicate AggreWell inserts in a simple and affordable way using PDMS (Sylgard) to reduce the porosity and reproducibility problems introduced by the agarose approach. Negative casts from Aggrewell inserts were created in 1.5% agarose, which were then filled with Sylgard 184 to create duplicates of the originals (Figure 4A-B). Sylgard is an affordable, non-porous, non-toxic, and optically clear PDMS elastomer. Additionally, Sylgard can be easily coated with polyethylene glycol (PEG) and poly(2-hydroxyethyl methacrylate) (pHEMA) to further inhibit cell adhesion and thus promote EB formation for further time and cost savings. H7 formed uniformly shaped and sized EBs in all substrates, with those in PEG-coated Sylgard showing a significant increase in EB size (Figure 4 C-E). EBs formed in Sylgard retained the ability to differentiate into all three germ layers (Figure 4F-J), with equal efficiency. Duplication of Aggrewell inserts using PEG-Sylgard-184 is affordable, reproducible, and scalable.

Task 3-5. Immunohistochemistry to verify upregulation of SGN-critical proteins and neurotrophin effects on electrical properties (months 1-18)

- These tasks rely on a reliable model of hPSCs. Progress from Task 2 indicates that the basic strategy produces excitable, glutamatergic neurons, but additional work on specifying an auditory phenotype is necessary before continuing with the histological and electrophysiological studies. We anticipate completing Tasks 3-5 in Year 2. Some preliminary data is provided below:
- Neurotransmitter fate: Neurons produced by the combination of RA and Pur positively labeled with vGlut1 (Figure 2G), indicating adoption of a glutamatergic fate. We found no positive staining to tyrosine hydroxylase, a marker of catecholamine production, or vGAT, a marker of GABAergic neurons (data not shown).
- Electrophysiology results: After two weeks in terminal differentiation media, neurons produced by the combination of RA and Pur exhibited voltage-gated sodium and potassium currents after two weeks in terminal differentiation media (data not shown). At this point, resting potentials were depolarized (approximately -20 mV) and current density was small. Only 1 of 20 cells exhibited overshooting action potentials. In preliminary experiments, cells exhibited no differential response to BDNF or NT3. We have not proceeded further since there will be modifications to the differentiation program in Year 2 to optimize differentiation of auditory neurons. After we maximize expression of otic markers, we will confirm expression of neurotrophic factor receptors and return to examination of electrophysiological traits in the presence and absence of BDNF and NT3, as outlined in Tasks 3-5.

Objective 2: Design a first-generation electrical interface for stimulation of stem cell-derived neurons grown on a nanofiber substrate. All tasks rely solely on cell lines (months 12-30)

Task 6. Minimize thickness of nanofiber mat to maximize flexibility (months 12-13)

- Due to the challenges and time necessary to accomplish hPSC reprogramming, we advanced in areas of Objectives 2 and 3. We have optimized electrospinning polystyrene nanofibers on a thin, even layer of poly(4-vinyl pyridine) (PVP). The PVP substrate will be required to obtain necessary dimensions for fiber implantation in deafened guinea pigs (see Objective 3, Task 14 for more details).

Tasks 7-12. Design, implement, and examine efficacy of electrical interface to nanofiber substrate (months 13-30)

- Pending tasks for Years 2-3

Objective 3: Optimize the integration of stem cell-derived neurons following *in vivo* transplantation of the seeded nanofibrous scaffold (months 18-48)

Task 13. Group 1: Pilot deafening. Confirm efficacy of β -bungarotoxin in guinea pig and time point of nerve death. 10 guinea pigs will be required, including an expected failure rate of 30% from morbidity and mortality (months 18-21)

- Following approaches in gerbil, we initially tested the efficacy of β -bungarotoxin-induced auditory neuropathy in guinea pig. Click-induced auditory brainstem responses (ABRs) were obtained for both ears prior to toxin introduction. Approximately 5 μ l of 0.05 μ g/ml β -bungarotoxin was applied to the round window niche of one ear. As shown in Figure 5, plastic sections revealed no pathology; click ABR thresholds and spiral ganglion neuron (SGN) counts were normal. Therefore, we examined another commonly reported ototoxin used for SGN degeneration, ouabain. About 5 μ l of a 10 mM solution was applied to the round window niche of one ear. We found a nearly complete loss of SGNs in basal and middle turns (Figure 5) as well as a profound shift in ABR threshold. Similar methods have recently been reported (Cho et al., 2011), but no normative data were provided on SGN loss by cochlear turn and, in contrast to our results, those authors reported no impact on sensory hair cells. We will establish a careful and systematic database of ouabain effects in the guinea pig ear that will be of broad use to other investigators exploring regenerative studies in the ouabain-treated guinea pig.

Task 14. Group 2: Pilot implantation. Confirm positional stability and integrity of implant over time. 15 guinea pigs will be required, including an expected failure rate of 30% from morbidity and mortality. No hiPSCs involved (months 21-27)

- Estimates of implant design constraints based on guinea pig anatomy indicated that a coiled nanofiber substrate, one that would mimic the topographical arrangement of the auditory ganglion, would need to be 0.2-0.4 μ m in diameter and between 2 and 5 mm in length. Traditional methods for rolling a nanofiber mat by coiling around a thin wire could only achieve one turn in no less than 1 mm diameter. The guinea pig auditory nerve is arranged in a 4-turn coil. Innovative methods were required to produce a self-rolling nanofibrous substrate that can be used to study nanofiber influence (as a 2D array for Objective 2) and regeneration (as a 3D coiled substrate for Objective 3).
- Conduit formation: Poly(4-vinyl pyridine) (PVP) was dissolved in chloroform at 3% (w/v) and used to form the bottom layer of the bilayer film. Polystyrene (PS) was dissolved at 3% (w/v) in toluene and used to form the top layer. The bottom layer was deposited on to the surface of a 22x22 mm cover glass and evenly thinned by spin-coating the solution at a speed of 2500 rpm with a ramping speed of 1000 rpm/s for 60s. After formation of the bottom was complete the layer was cross-linked by UV radiation using a radiation dose of \sim 4 J/cm². Polystyrene was deposited and spun using the same spin-coating parameters. The two layers were then cross-linked together using the same radiation dose. The bilayer films were cut in to vertical strips \sim 3 mm x 22 mm vertical strips using a razor blade. The bilayers were submerged in 0.1% 1 M HCl in order to facilitate rolling of the polymer films. Rolled polymer conduits were allowed to roll until they reached a diameter of 150-200 μ m (Figure 6A). Up to 8 complete revolutions could be obtained (Figure 6B).
- Electrospinning: 1.6 g of PS was dissolved in 7 ml dichloromethane (DCM), about 24% w/v. After all of the PS was completely dissolved, 3 ml of dimethylformamide (DMF) was added to the solution. The solution was loaded to a 3 ml syringe with a 22 gauge blunt-tip needle and placed on a syringe pump set

to 0.25 ml/hour. The tip of the needle was protruded through the center of a 10x10 cm folded aluminum sheet. The rotating disc collector was placed 35 cm away such that the axis of rotation was perpendicular to the syringe. A high voltage power supply applied a 20 kV charge to the aluminum sheet via an alligator clip. A second power supply applied a counter charge of -2kV to the rotating disc via a wire brush. Fibers were collected for 5 minutes or until a desired density was obtained. Electrospun fibers could be captured on the PVP conduit (Figure 6C). Rolled conduits (without fibers) were cut to ~2 mm in length to explore surgical approaches (Figure 6D).

- **Surgical approach:** We used guinea pig temporal bones to develop the surgical approach for implantation within the internal auditory meatus (IAM). In Figure 7A, we show the lateral wall of an intact guinea pig bone and mark the drilling location that will give us access to the middle and inner ear. The linear distance between this spot and the brainstem is estimated to be approximately 3.5 mm. After opening the middle ear, a second fenestra will be required to gain access to the modiolus (Figure 7B) and the IAM (Figure 7C). The IAM is about 0.45 mm in cross section but is highly vascularized. The final position of the scaffold, about 0.2 mm in diameter, is illustrated in Figure 7D.
- In Year 2, we will examine placement in live animals and test for electrical ABR response using a single thin electrode placed alongside the scaffold in the IAM.

Tasks 15 through 18 examine the functional integration of hiPSC-derived neurons following implantation of the neuralized nanofibers.

- Pending tasks for Years 2-4

B. REPORTABLE OUTCOMES

Abstracts

1. **Duncan RK**, Liu L, Schaefer S, Decker M (2014) Serum-free and feeder-free derivation of human neural progenitors with fasciculated architectures. Abstracts of the 37th MidWinter Meeting of the Association for Research in Otolaryngology, accepted.
2. Schaefer S, Varma S, **Duncan RK** (2014) Micropatterned silicone substrates for affordable and reproducible embryoid body formation. Abstracts of the 37th MidWinter Meeting of the Association for Research in Otolaryngology, accepted.

Development of cell lines

Human pluripotent stem cell lines stably expressing Neurog1, either constitutively or inducible, are currently being developed.

Databases

We have generated a normative database of the number spiral ganglion neurons in the normal and ouabain treated guinea pig. These normative data will form the reference for determining the extent of new neural growth in the implanted deafened ear.

Research opportunities applied for based on experience supported by this award

Experience in nanofiber scaffold design and stem cell differentiation garnered during the past year has facilitated an application by our co-investigator Dr. Joseph Corey to the VA BLRD entitled “Accelerating the growth of motor axons using mechanical tension.” There is no scientific overlap with the current award.

C. CONCLUSION

The research completed to date shows that simple overexpression of Neurog1 is a less efficient method for generating stem cell-derived neurons using hESCs compared with prior work in mESCs. This could reflect basic differences between mouse and human or simple differences in two separate stem cell lines. Regardless, a more robust method for generating auditory nerve-like cells is required, particularly one that can be easily translated to a variety of human pluripotent stem cell lines. We have shown that combinations of retinoic acid

and purmorphamine pattern stem cells toward a sensory placodal fate and that adenoviral delivery of Neurogenin-1 can dramatically increase the expression of this proneural gene. Further study needs to be conducted to examine the impact of Ad5.Neurog1 overexpression on the maturation and excitability of the derived neurons, as well as on the expression of mature auditory nerve markers. In developing this approach, we have also produced a reliable and affordable method for generating spin-aggregated embryoid bodies. This method will open new avenues in stem cell and cancer research, providing an easy and scalable method for generating micropatterned PDMS substrates.

Our advanced studies on nanofiber scaffold design have provided a unique and novel method for self-rolling nanofibrous substrates. While scaffolds have been in use for nerve grafts for some time, none have been generated on this size scale in a tubular format and none provide the concentric topology that may be of considerable advantage in restricting the migration of incorporated cells. Most peripheral neural tracks are characterized by a topographical arrangement such that central and lateral neurons in a ganglion target unique cells. Thus, the coiled substrate may be of broad value to the regeneration field. Moreover, achieving coiled substrates on sub-millimeter diameter scales opens new avenues of research and paves the way for a viable auditory nerve graft.

D. REFERENCES

- Cho YB, Cho HH, Jang S, Jeong HS, Park JS (2011) Transplantation of neural differentiated human mesenchymal stem cells into the cochlea of an auditory-neuropathy guinea pig model. *J Korean Med Sci* 26:492-498.
- Dahlmann J, Kensah G, Kempf H, Skvorc D, Gawol A, Elliott DA, Drager G, Zweigerdt R, Martin U, Gruh I (2013) The use of agarose microwells for scalable embryoid body formation and cardiac differentiation of human and murine pluripotent stem cells. *Biomaterials* 34:2463-2471.
- Hashino E, Fritsch MH (eds.) (2011) Embryonic stem cell-derived neurons for inner ear therapy: InTech.
- Hester ME, Murtha MJ, Song S, Rao M, Miranda CJ, Meyer K, Tian J, Boulting G, Schaffer DV, Zhu MX, Pfaff SL, Gage FH, Kaspar BK (2011) Rapid and efficient generation of functional motor neurons from human pluripotent stem cells using gene delivered transcription factor codes. *Mol Ther* 19:1905-1912.
- Hill GW, 3rd, Purcell EK, Liu L, Velkey JM, Altschuler RA, Duncan RK (2012) Netrin-1-mediated axon guidance in mouse embryonic stem cells overexpressing neurogenin-1. *Stem Cells Dev* 21:2827-2837.
- Kim JE, O'Sullivan ML, Sanchez CA, Hwang M, Israel MA, Brennand K, Deerinck TJ, Goldstein LS, Gage FH, Ellisman MH, Ghosh A (2011) Investigating synapse formation and function using human pluripotent stem cell-derived neurons. *Proc Natl Acad Sci U S A* 108:3005-3010.
- Ma Q, Anderson DJ, Fritsch B (2000) Neurogenin 1 null mutant ears develop fewer, morphologically normal hair cells in smaller sensory epithelia devoid of innervation. *J Assoc Res Otolaryngol* 1:129-143.
- Norrmann K, Fischer Y, Bonnamy B, Wolfhagen Sand F, Ravassard P, Semb H (2010) Quantitative comparison of constitutive promoters in human ES cells. *PLoS One* 5:e12413.
- Purcell EK, Naim Y, Yang A, Leach MK, Velkey JM, Duncan RK, Corey JM (2012) Combining topographical and genetic cues to promote neuronal fate specification in stem cells. *Biomacromolecules* 13:3427-3438.
- Purcell EK, Yang A, Liu L, Velkey JM, Morales MM, Duncan RK (2013) BDNF profoundly and specifically increases KCNQ4 expression in neurons derived from embryonic stem cells. *Stem Cell Res* 10:29-35.
- Schlosser G (2006) Induction and specification of cranial placodes. *Dev Biol* 294:303-351.
- Tong M, Hernandez JL, Purcell EK, Altschuler RA, Duncan RK (2010) The intrinsic electrophysiological properties of neurons derived from mouse embryonic stem cells overexpressing neurogenin-1. *Am J Physiol Cell Physiol* 299:C1335-1344.

SUPPORTING DATA

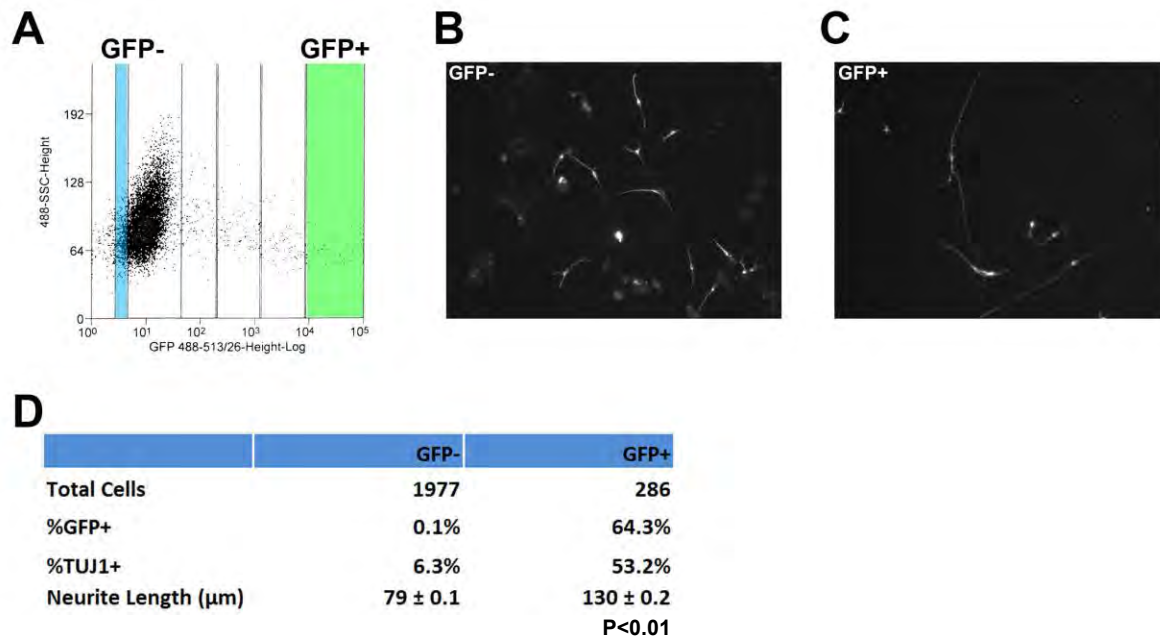


Figure 1: Effects of EF1 α .Neurog1.IRES.GFP plasmid expression in hESCs. (A) Flow cytometry analysis to identify GFP+ and GFP- cells. The large cluster of cells on the left represent the GFP- cells and exhibited similar attributes to untransfected control cells. Ten percent of the least fluorescent cells in this group were gated as GFP-. GFP-expressing cells were binned in quartiles and the brightest 25% were gated as GFP+. (B) GFP- and (C) GFP+ cells were plated at a concentration of 60,000 cells per well in a 6-well dish, cultured for 5 days in terminal differentiation media, stained for TUJ1, and examined. (D) Over 30 randomly selected regions were examined and cell data quantified, including total cell number, %GFP+, %TUJ1+, and major neurite length. Even after 5 days, many GFP+ cells were still expressing the marker and a majority of these were TUJ+. Neurites in the GFP+ culture were significantly longer than those spontaneously differentiated neurons in the GFP-group.

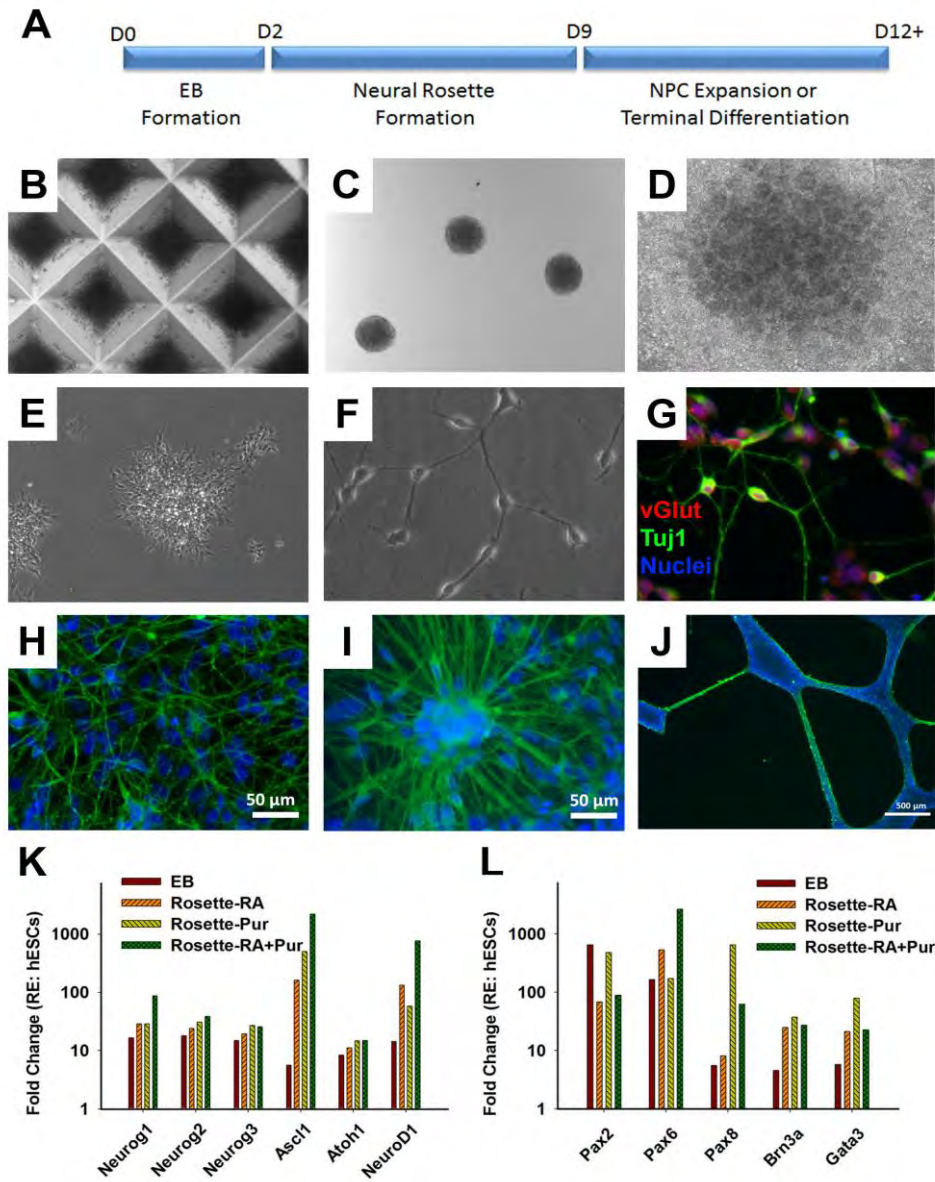


Figure 2: Small molecule morphogen strategy for generating glutamatergic sensory neurons.

(A) A cartoon of the general scheme is shown. From D0 to D2, embryoid bodies are formed in Aggrewell 800 microwells in the presence of SMAD inhibitors noggin and dorsomorphin to produce a neuroectodermal lineage. Embryoid bodies are grown on Matrigel for 7-8 additional days to produce neural rosettes. Rosettes are formed in the presence of retinoic acid (RA) and/or the sonic hedgehog agonist purmorphamine (Pur). Rosettes are collected and cells isolated for expansion of neural progenitor cells (NPCs) or terminal differentiation in Neurobasal supplemented with N2 and B27. Examples are shown for (B) Aggrewell aggregates, (C) free-floating embryoid bodies, (D) neural rosettes, (E) NPCs, and (F) terminal differentiated neurons. (G) After two-weeks in terminal differentiation culture, cells label positive for vGlut1, indicating a glutamatergic fate. High-density cultures at this 2-week time point exhibited several distinct morphologies including (H) extensive networks, (I) fasciculations, and (J) large-scale 3D aggregates of neural clusters. (K) Quantitative PCR revealed broad upregulation of bHLH genes even at the embryoid body (EB) stage. The presence of RA and/or Pur had little effect on neurogenins, except a 10-fold increase in Neurog1 for the RA+Pur condition. In contrast, both morphogens had a large impact on Ascl1. (L) Purmorphamine had the largest impact on otic transcriptional cascades (Pax2/8-Brn3a-Gata3), but the lens/olfactory marker Pax6 was also highly upregulated by this paradigm.

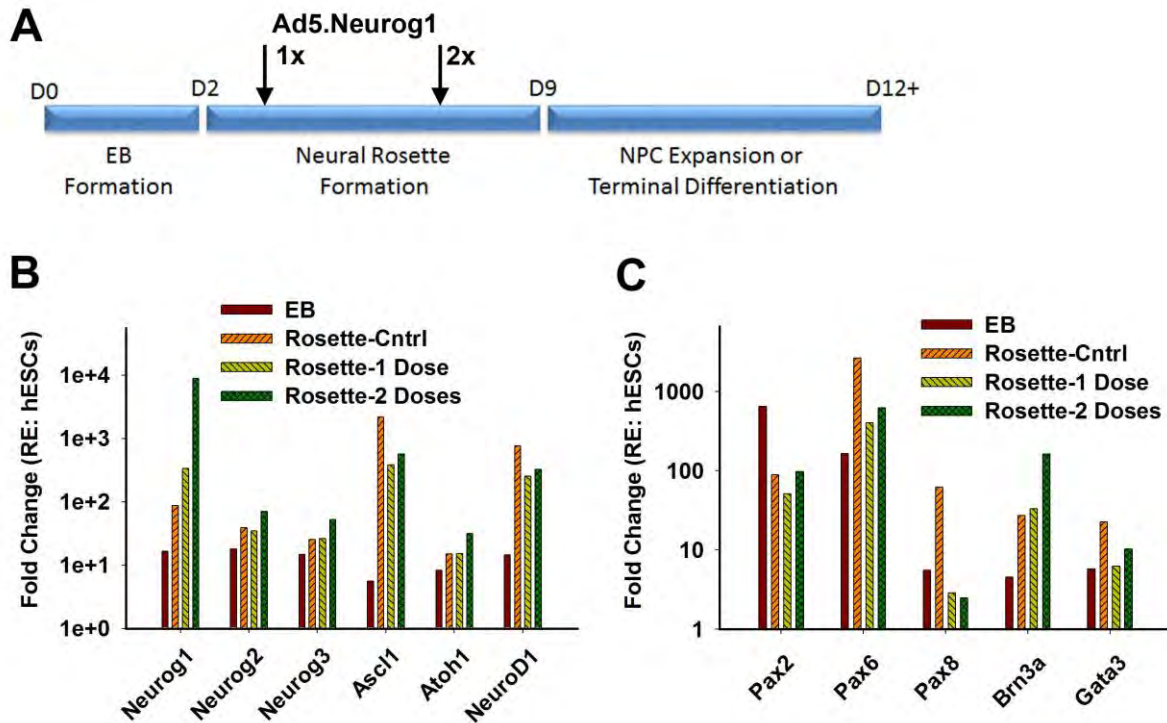


Figure 3: Effects of Ad5.Neurog1 infection in pre-differentiated hPSCs. (A) A cartoon of the reprogramming strategy is shown with arrows pointing to D3 and D7 timepoints for first and second virus exposures. (B) Quantitative PCR data is shown for EBs and D9 rosettes after one or two doses of adenovirus. All rosettes were exposed to RA and Pur (see Figure 2). Virus infection dramatically increased expression of Neurog1 with little impact on other neurogenin family members. Interestingly, expression of the bHLH gene *Ascl1* decreased in response to Ad5.Neurog1. *NeuroD1* was marginally affected. (C) Surprisingly, with the exception of *Brn3a* after 2 doses of virus, the overexpression of Neurog1 did not significantly increase the expression of otic transcription factors.

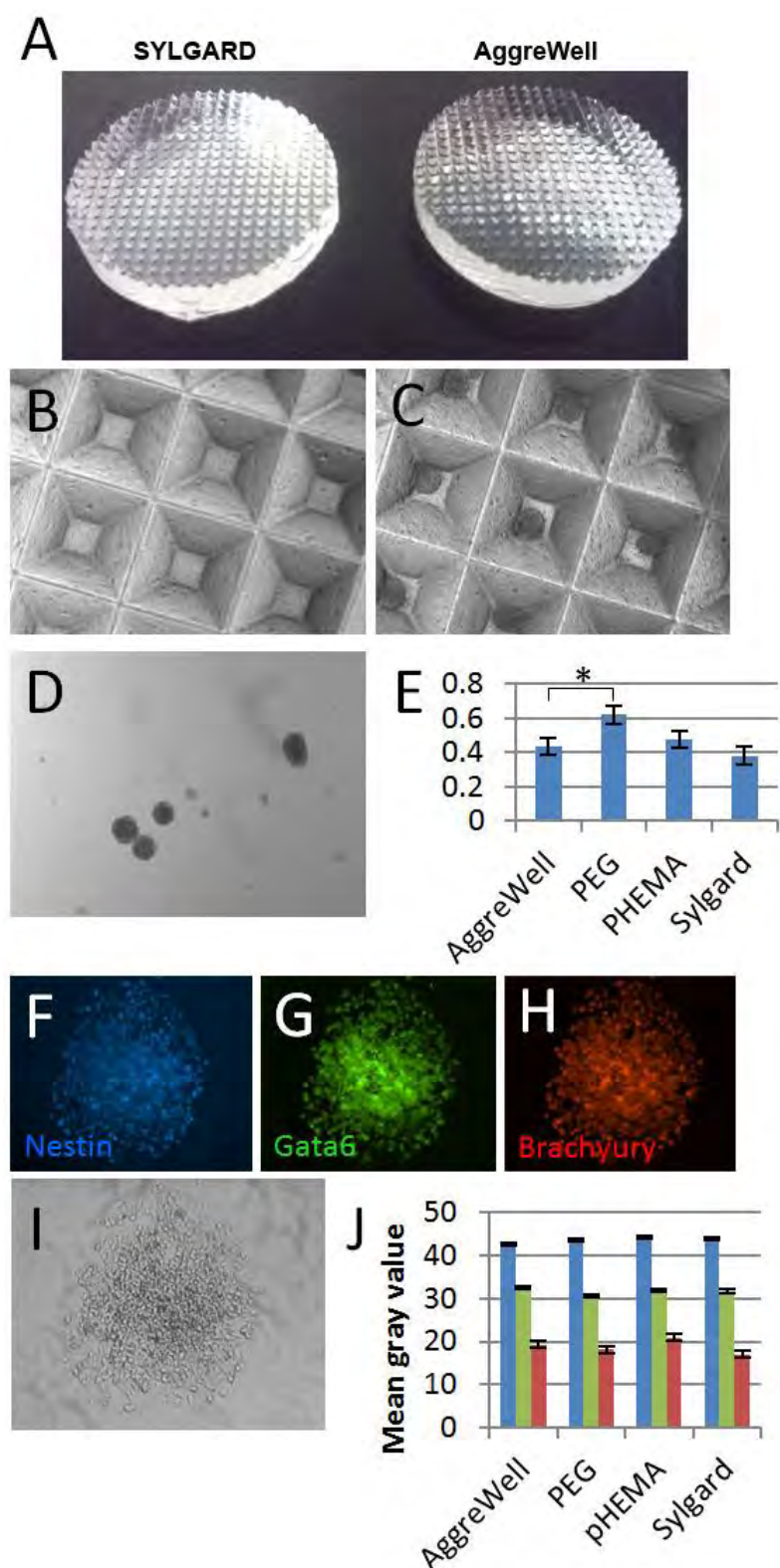


Figure 4: Sylgard microwell culture inserts and formation and staining of EBs. (A) Comparison of Sylgard and original AggreWell substrate. (B) Sylgard insert seeded with 225,000 cells (750 cells per EB). (C) EBs after 48 hours within microwells. (D) EBs in suspension at harvest. (E) Quantification of average sizes of EBs formed on AggreWell versus coated or uncoated Sylgard. (F-H) Representative immunofluorescence staining for embryonic lineage markers. (I) Bright field image of EB attached to Matrigel substrate for staining. (J) Quantification of immunofluorescence signal from EBs formed on various culture inserts.

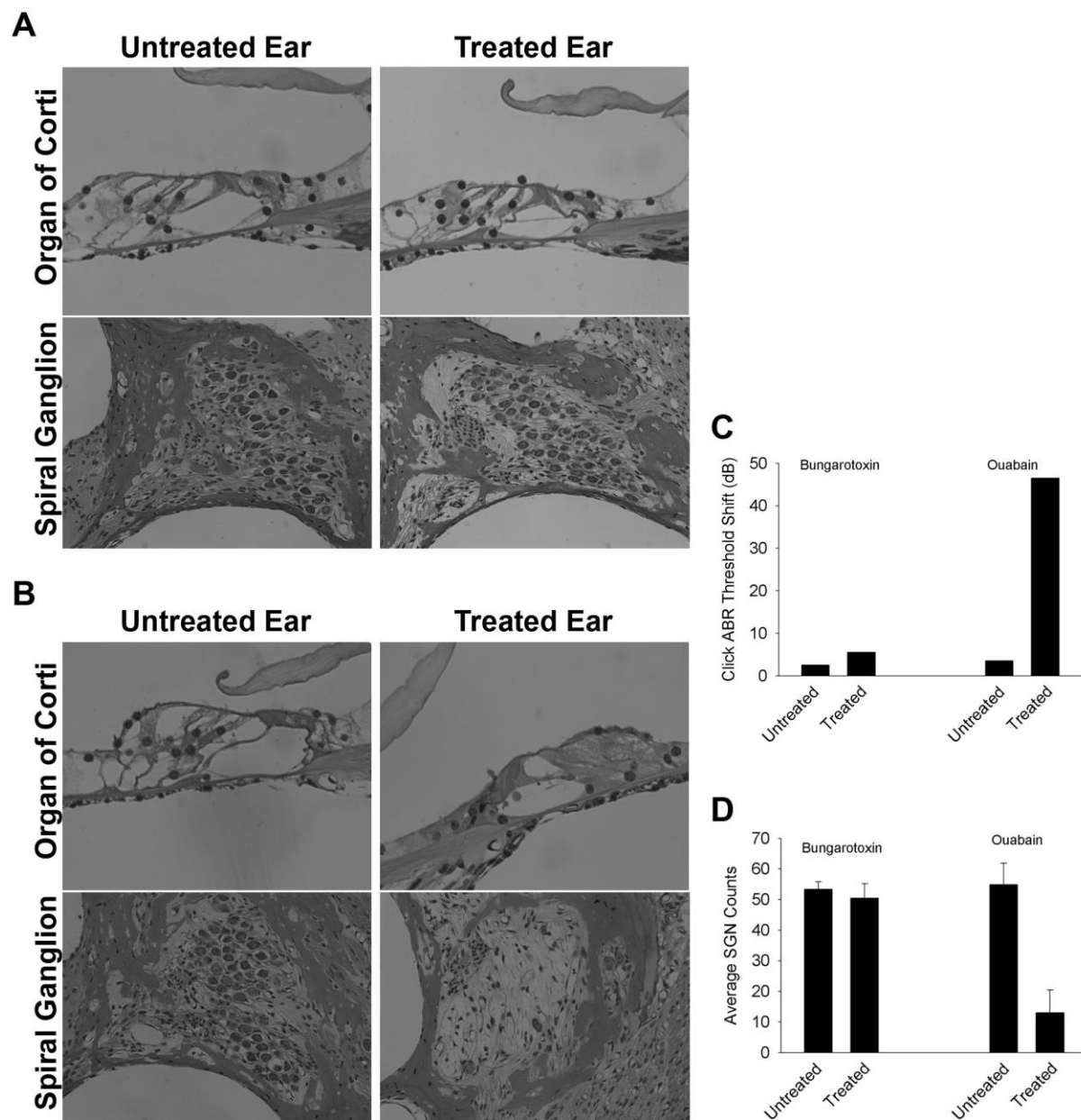


Figure 5: Comparison of β -bungarotoxin and ouabain to produce auditory neuropathy in guinea pigs. Plastic sections from mid-cochlear turns for (A) β -bungarotoxin and (B) ouabain treated ears compared to contralateral ear controls. Only the ouabain treatment revealed substantial loss of spiral ganglion cells, as well as loss to sensory hair cells. (C) Ouabain resulted in significant threshold shift in click auditory brainstem responses (ABR) 2-weeks after treatment. (D) Ouabain caused a significant decrease in average spiral ganglion neuron (SGN) number ($P < 0.05$), whereas β -bungarotoxin had no effect on hearing thresholds or SGN count. Data in panel C are representative of two separate guinea pigs for each treatment condition.

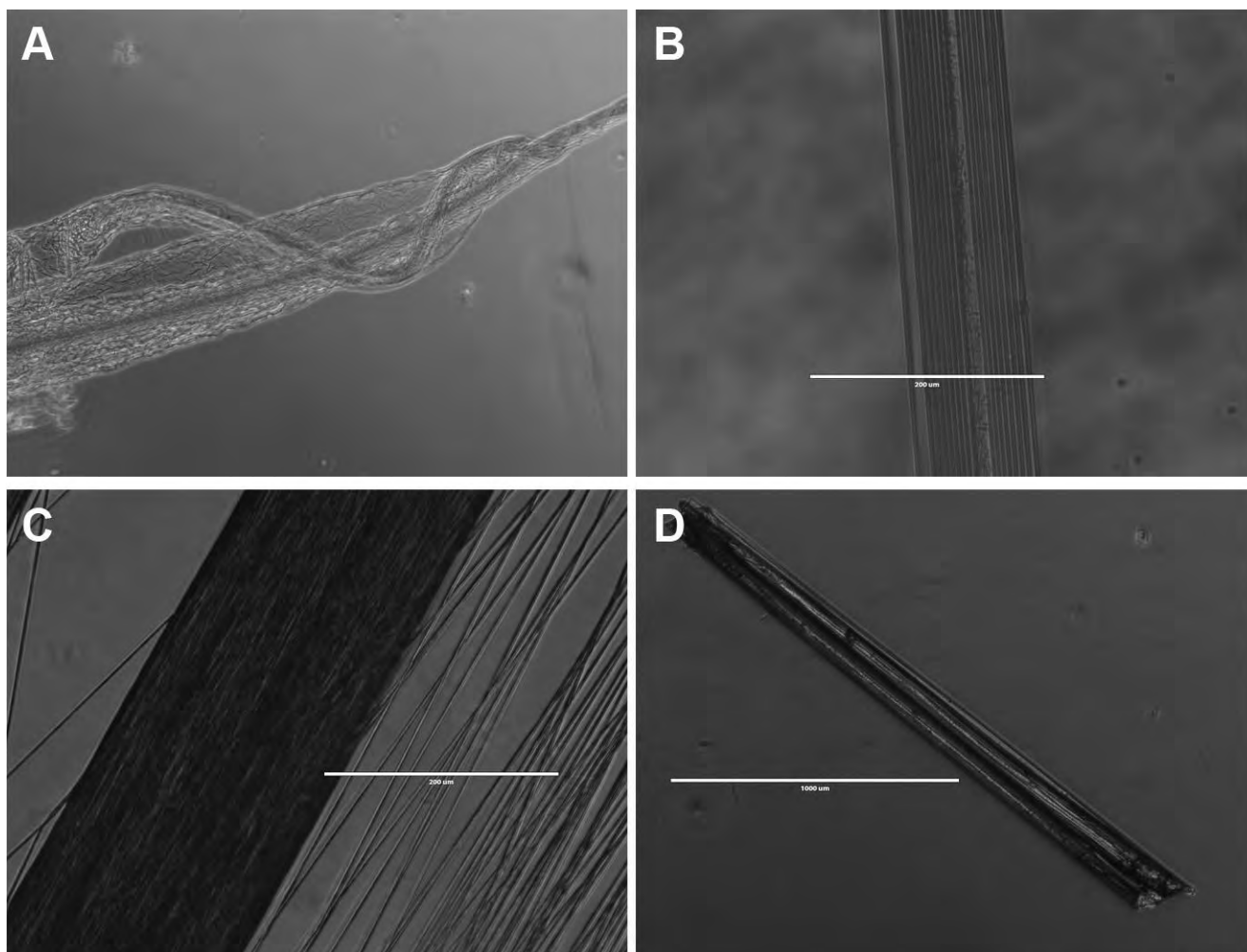


Figure 6: Self-rolling nerve guidance channel designed and constructed to accommodate narrow nerves. (A) Conduits are constructed from a monolayer film consisting of 3% wt of poly(4-vinyl pyridine) (PVP) crosslinked by a short UV light exposure. In the photograph, the conduit forms a cone structure at the end (upper right), revealing a concentric formation of the conduit. (B) A concentric self-rolled conduit constructed from a bilayer of PVP (bottom layer) crosslinked to 3% wt polystyrene (PS) (upper layer). This longitudinal view of a conduit shows 8 visible concentric layers. (C) Integration of electrospun nanofibers into self-rolling conduit. Some PVP-PS bilayers were placed on a rotating disc to collect aligned PS nanofibers surface before rolling of the conduit was allowed. The rolling film (opaque structure on the left) encapsulated fibers in its path of rotation to the right. Some nanofibers on the right side of the photograph were not encapsulated. (D) PVP-PS films continued to roll to a final diameter of 150-200 μm . The conduits were cut to a length of 2 mm.

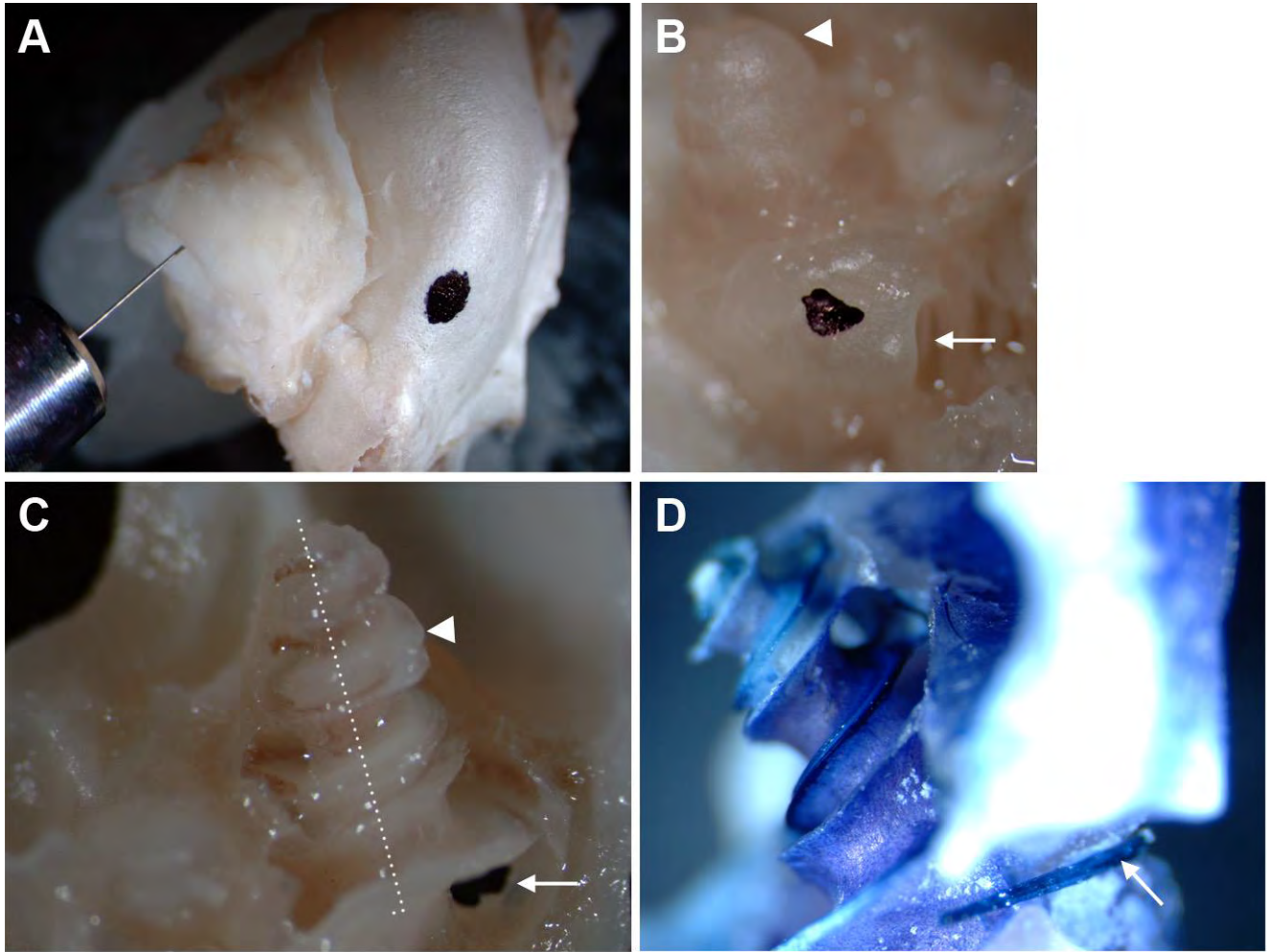


Figure 7: A surgical approach has been developed for the placement of the biopolymer scaffold within the internal auditory meatus (IAM) of the guinea pig. (A) The lateral wall of an intact guinea pig temporal bone is shown. A fine wire is inserted into the external auditory meatus for orientation. The area of the bullar wall covering the middle ear is marked (ink spot) where a fenestra will be drilled to provide access to the middle and inner ear. (B) The middle ear has been widely opened, revealing the intact otic capsule covering the cochlea. An area marking the site of a much smaller fenestra (1 – 2 mm) for implantation is shown (ink spot). The fenestra will expose the modiolar bone that houses the spiral ganglion cells and axons forming the auditory nerve. The membrane covered round window (arrow) and the apex of the cochlea (arrowhead) are indicated for orientation. (C) The bony cochlear duct has been microdissected to expose each turn of the organ of Corti containing the sensoriepithelium of the cochlea (arrowhead) and the spiral modiolus containing the auditory nerve (dotted line). In the scala tympani of the basal turn, a hole (arrow) has been created leading into the modiolus at the point where it curves to form the IAM, through which the auditory nerve then travels to the brain stem auditory nuclei. This hole lies directly under the site of the otic capsule fenestra shown in (B). (D) A cross-section of the IAM with scaffold (arrow) is shown. Both have been dyed to provide contrast and detail. It is through the two fenestra, first through the otic capsule into the cochlea and then through the modiolus exposing the entrance to the IAM, that the nanofiber scaffold will be placed, as shown.